0026-895X/07/7206-1447–1456$20.00
MOLECULAR PHARMACOLOGY
Copyright © 2007 The American Society for Pharmacology and Experimental Therapeutics
Mol Pharmacol 72:1447–1456, 2007

Vol. 72, No. 6
35980/3274085
Printed in U.S.A.

Evidence for Functional $P2X_4/P2X_7$ Heteromeric Receptors[S]

Chang Guo, Marianela Masin, Omar S. Qureshi, and Ruth D. Murrell-Lagnado

Department of Pharmacology, University of Cambridge, Cambridge, United Kingdom

ABSTRACT

The cytolytic ionotropic ATP receptor $P2X_7$ has several important roles in immune cell regulation, such as cytokine release, apoptosis, and microbial killing. Although $P2X_7$ receptors are frequently coexpressed with another subtype of P2X receptor, $P2X_4$, they are believed not to form heteromeric assemblies but to function only as homomers. Both receptors play a role in neuropathic pain; therefore, understanding how they coordinate the cellular response to ATP is important for the development of effective pain therapies. Here, we provide biochemical and electrophysiological evidence for an association between $P2X_4$ and $P2X_7$ that increases the diversity of receptor currents mediated via these two subtypes. The heterologously expressed receptors were coimmunoprecipitated from human embryonic kidney (HEK) 293 cells, and the endogenous $P2X_4$ and $P2X_7$ receptors were similarly coimmunoprecipitated from bone marrow-derived macrophages. In HEK293 cells, the fraction of $P2X_4$ receptors biotinylated at the plasma membrane increased 2-fold in the presence of $P2X_7$ although there was no change in overall expression. Coexpression of a dominant-negative $P2X_4$ mutant (C353W) with $P2X_7$, inhibited $P2X_7$ receptor mediated currents by greater than 2-fold, whereas a nonfunctional but non–dominant-negative mutant (S341W) did not. Coexpression of $P2X_4$S341W with $P2X_7$ produced a current that was potentiated by ivermectin and inhibited by 2′,3′-*O*-(2,4,6-trinitrophenyl) adenosine 5-triphosphate (TNP-ATP), whereas expression of $P2X_7$ alone produced a current that was insensitive to both of these compounds at the concentrations used. These results demonstrate a structural and functional interaction between $P2X_4$ and $P2X_7$, which suggests that they associate to form heteromeric receptors.

Extracellular ATP acts as a signaling molecule exerting effects on a range of biological functions including immune regulation, apoptosis, cellular proliferation, and neurotransmission (Khakh and North, 2006). P2X receptors are cationic channels gated by extracellular ATP, of which seven subtypes have been identified that assemble as either homo- or heterotrimeric receptors (North, 2002; Barrera et al., 2005; Nicke et al., 2005; Ormond et al., 2006). Heteromerization can change both the functional and pharmacological properties of P2X receptors (Lewis et al., 1995; King et al., 2000). One member of this family, $P2X_7$ receptor, is believed to be unique among P2X receptors in only forming homomeric assemblies (Torres et al., 1999).

Activation of $P2X_7$ receptors, which are expressed in a range of immune cells, can result in the release of IL-1β, IL-18, tumor necrosis factor -α, and matrix metalloproteinase 9, activation of the stress-activated protein kinase/c-Jun NH_2-terminal kinase pathway, membrane blebbing, and apoptotic or necrotic cell death (Humphreys et al., 2000; Perregaux et al., 2000; Wilson et al., 2002; Gu and Wiley, 2006). This receptor represents an important target in inflammatory diseases such as arthritis, neuropathic pain, and stroke (Dell'Antonio et al., 2002; Labasi et al., 2002; Chessell et al., 2005). In immune cells such as macrophages, monocytes, and microglia, $P2X_7$ receptors are coexpressed with another member of the P2X family also important in neuropathic pain, the $P2X_4$ receptor (Bowler et al., 2003; Xiang and Burnstock, 2005). The role of this receptor in immune cells is not as well understood; however, it has considerably higher affinity for ATP than the $P2X_7$ receptor, and its up-regulation in spinal cord microglia as a result of peripheral nerve injury contributes to allodynia type hypersensitivity (Tsuda et al., 2003).

Coexpression of $P2X_4$ and $P2X_7$ is not restricted to immune cells. They are also present together in endothelial and epithelial cells, and a recent electrophysiological study of P2X receptors that are present in ciliated airway epithelia and are believed to be important for mucociliary clearance reported

This work was supported by the Biotechnology and Biological Sciences Research Council.

Article, publication date, and citation information can be found at http://molpharm.aspetjournals.org.

doi:10.1124/mol.107.035980.

[S] The online version of this article (available at http://molpharm.aspetjournals.org) contains supplemental material.

ABBREVIATIONS: IL, interleukin; BzATP, 2′,3′-*O*-(benzoyl-4-benzoyl)-adenosine 5-triphosphate; NP-40, Nondiet P-40; EGFP, enhanced green fluorescent protein; ER, endoplasmic reticulum; FITC, fluorescein isothiocyanate; HA, hemagglutinin; HEK, human embryonic kidney; NRK, normal rat kidney; BMDM, bone marrow derived macrophage; PBS, phosphate-buffered saline; PAGE, polyacrylamide gel electrophoresis; TNP-ATP, 2′,3′-*O*-(2,4,6-trinitrophenyl) adenosine 5-triphosphate; BBG, Brilliant Blue G; EC, extracellular; wt, wild type; PFA, paraformaldehyde; DDM, *n*-dodecyl-*b*-D-maltoside; HRP, horseradish peroxidase; IVM, ivermectin; CHAPS, 3-[(3-cholamidopropyl)dimethylammonio]propanesulfonate; HBS, HEPES-buffered saline.

currents with a novel combination of both $P2X_7$ and $P2X_4$ receptor characteristics (Ma et al., 2006). By comparing amino acid sequences, it was found that $P2X_4$ is more homologous to $P2X_7$ (~40%) than are the other P2X receptor subtypes; however, a previous coimmunoprecipitation study with heterologously expressed receptors failed to provide evidence for the formation of stable $P2X_{4/7}$ complexes (Torres et al., 1999).

To understand how receptors transmit an ATP signal, we need to define the subunit identity of the physiological receptors. The formation of a $P2X_{4/7}$ heteromer could provide an important mechanism for the modulation of $P2X_7$ receptor signaling and so has important consequences for $P2X_7$ as a therapeutic target and for its physiological roles in a range of diseases and immune cell function. We sought to evaluate a molecular basis for its existence using biochemical, functional, and pharmacological methods.

Materials and Methods

Antibodies and Reagents. The following primary antibodies were used: rabbit polyclonal anti-$P2X_2$ subunit (0.6 μg/ml; Alomone Labs, Jerusalem, Israel), rabbit polyclonal anti-$P2X_4$ subunit (6 μg/ml; Alomone Labs), rabbit polyclonal anti-$P2X_7$ subunit (1.5 μg/ml; Alomone Labs), mouse monoclonal anti-hemagglutinin (HA) (0.8 μg/ml; Roche, Indianapolis, IN), rabbit polyclonal anti-EE (1 μg/ml; Bethyl Laboratories, Cambridge, UK), anti-LAMP-1 (0.8 μg/ml; Santa Cruz Biotechnology, Santa Cruz, CA). FITC- or Cy3-conjugated goat anti-mouse or anti-rabbit IgG secondary antibodies (1:250; Jackson ImmunoResearch Laboratories, Inc., West Grove, PA) were used for immunofluorescence. Horseradish peroxidase-conjugated anti-mouse or anti-rabbit secondary antibodies (1:10,000; GE Healthcare, Chalfont St. Giles, Buckinghamshire, UK, and Perbio Science, Cramlington, UK) or Rabbit TrueBlot-Horseradish Peroxidase (HRP) anti-rabbit IgG (eBioscience, San Diego, CA) were used for Western blotting. Complete Protease Inhibitor cocktail (Roche), *n*-dodecyl-*b*-D-maltoside (DDM; Melford Laboratories, Ipswich, Suffolk, UK), anti-rabbit IgG beads (eBioscience), and BCA Protein assay kit (Pierce, Rockford, IL) were used for coimmunoprecipitation experiments. Sulfo-succinimidyl 2-(biotinamido)-ethyl-1,3′-dithiopropionate was from Pierce. Unless otherwise stated, all others reagents were obtained from Sigma (St. Louis, MO) or Invitrogen (Carlsbad, CA).

DNA Constructs. The construction and characterization of $P2X_4$ and $P2X_2$ receptors with enhanced green fluorescent protein fused to the C terminus ($P2X_4$-EGFP, $P2X_2$-EGFP) has been described previously (Bobanovic et al., 2002). In brief, to generate cDNA encoding $P2X_4$ with EGFP fused to the C terminus, the rat cDNA (a kind gift from Dr. P. P. A. Humphrey) was amplified by polymerase chain reaction using oligonucleotide primers to introduce a Kozak initiation sequence (Kozak, 1987) to remove the stop codon and to introduce NheI and SacII sites at the 5′ and 3′ ends, respectively. Amplification products were then cloned into the pEGFP-N1 vector (BD Biosciences Clontech, Palo Alto, CA). Other constructs used include wild-type $P2X_4$ and $P2X_4$ with a HA tag at the C terminus. These sequences were subcloned into the pEGFP-N1 vector so that the enhanced green fluorescent protein (EGFP) sequence was excised. The C353W and S341W point mutations were made using the QuikChange II site-directed mutagenesis kit (Stratagene, La Jolla, CA) in $P2X_4$-EGFP. The sequences of all amplified regions were verified using automated DNA sequencing (Department of Genetics, University of Cambridge, Cambridge, UK). Other constructs used include wild-type rat $P2X_7$ and $P2X_2$, $P2X_2$ tagged at its N terminus with HA, pEGFP-N1, and DsRed-ER (BD Biosciences Clontech). Glu-Glu (EE)-tagged $P2X_7$ in pcDNA3 was a kind gift from A. Surprenant.

Cell Culture and Transfection. Normal rat kidney (NRK) cells and human embryonic kidney (HEK) 293 cells were maintained in Dulbecco's modified Eagle's medium containing 10% fetal bovine serum and 100 U/ml penicillin/streptomycin at 37°C and 5% CO_2. Transient transfections of NRK cells were carried out using Lipofectamine 2000 (Invitrogen) according to the manufacturer's instructions. For transfection of one well of a 12-well plate, 1 μg of plasmid DNA was used. Transient transfections of HEK293 cells were carried out using the modified calcium phosphate method as described previously (Bobanovic et al., 2002). The amount of DNA used to form a precipitate was 3 μg (in 100 μl of $CaCl_2$/100 μl of 2× HBS), and this was added to cells (200 μl/well) for 6 h. For cotransfection experiments, equal amounts of DNA were used, and we also included 0.5 μg of pEGFP-N1 vector for coexpression of EGFP with nonfluorescent constructs.

Bone marrow-derived macrophages (BMDMs) were obtained from 5- to 6-week-old male CD-1 mice. Mice were killed, the femur was excised, and the epiphyses were removed before flushing out the bone marrow. Cells were washed and resuspended in RPMI 1640 media supplemented with 20% fetal calf serum, 100 U/ml penicillin/streptomycin, and 30% L929 cell-conditioned media. Cells were cultured for 7 days before use and were treated for 48 h with lipopolysaccharide solution (1 μg/ml) before membrane protein fraction isolation.

Cell Biology and Immunofluorescence Protocols. Both NRK and HEK293 cells were plated onto poly(D-lysine)-treated coverslips. All cells were used 24 h after transfection. The basic protocol for total staining of the receptors was as follows. Cells were fixed in 3% paraformaldehyde (PFA) and 4% sucrose in PBS (1.5 mM NaH_2PO_4, 8 mM Na_2HPO_4, and 145 mM NaCl, pH 7.3) for 10 min at 4°C. If required, permeabilization was done using 0.1% Triton X-100 in PBS for 10 min at 4°C. Nonspecific sites were blocked using PBS containing 4% normal goat serum and 3% bovine serum albumin (blocking buffer). Antibodies were diluted to their final concentration in blocking solution. Primary antibodies were applied for 2 h at room temperature. Cells were rinsed once in blocking buffer and three times for 5 min with PBS, and then secondary antibodies were applied for 2 h at room temperature. Finally, cells were washed five times for 5 min with PBS and mounted onto slides with Vectashield (Vector Laboratories, Burlingame, CA) as a mounting medium. In some experiments, 100% methanol was used for 10 min at −20°C to fix and permeabilize the cells.

Image Analysis. Fluorescence was visualized using a Zeiss Axiovert LSM510 confocal microscope using a 63× oil immersion objective (Carl Zeiss Inc., Thornwood, NY). For FITC-Cy3 anti-FLAG double labeling, FITC and Cy3 were excited at 7 and 60% of 488 and 543 laser power, respectively. For each experiment, images were collected using identical acquisition parameters and analyzed using Image J. Pixel values were on an 8-bit scale ($2^8 = 256$; 0–255).

Biotinylation. Cells were washed with ice-cold PBS and incubated with 1 mg/ml sulfo-succinimidyl 2-(biotinamido)-ethyl-1,3′-dithiopropionate for 20 min at 4°C. Excess biotin was quenched with PBS containing 50 mM glycine. Cells were solubilized with lysis buffer (20 mM Tris, pH 8.0, 150 mM NaCl, 1 mM EDTA, 2 mM EGTA, 1% NP-40, 1 mM phenylmethylsulfonyl fluoride, 50 mM NaF, 1 mM sodium orthophosphate, 20 mM β-glycerophosphate, 10 mM sodium pyrophosphate, and protease inhibitors) and incubated on ice for 30 min, after which time they were sonicated and cleared by centrifugation. The majority of the supernatant was incubated with immobilized NeutrAvidin biotin binding protein beads (Pierce) on a rotating rack for 2 h at 4°C to precipitate biotinylated proteins. The remaining supernatant was kept to assess total protein in each sample. Beads containing precipitated biotinylated proteins were spun for 1 min at 10,000 rpm at 4°C and washed at least three times. The protein was eluted from the beads by incubation in 20 μl of the Laemmli buffer. Proteins were separated by SDS-PAGE by loading on 7.5% polyacrylamide gels and detected by immunoblotting. The $P2X_4$ receptor was detected using a rabbit polyclonal anti-$P2X_4$

antibody (1:500). The $P2X_7$ receptor was detected using a rabbit polyclonal anti-$P2X_7$ antibody (1:100). Immunoreactive bands were visualized using appropriate horseradish peroxidase-conjugated secondary antibodies followed by enhanced chemiluminescence detection. All blots shown in figures are typical of at least two and, in most cases, four similar results.

Membrane Protein Fraction Isolation. To obtain total membrane protein fractions for immunoprecipitation assays, transfected HEK293 cells or BMDMs were washed three times with HBS-EDTA buffer (50 mM HEPES pH 7.4, 100 mM NaCl, and 2 mM EDTA), scraped off, and then collected by gentle centrifugation. The cell pellet was resuspended in ice-cold hypotonic buffer (10 mM Tris-HCl pH 7.0, 2 mM EDTA, 1 mM phenylmethylsulfonyl fluoride, and Protease Inhibitors cocktail) and incubated for 20 min on ice. Cells were mechanically disrupted by passing the solution through a needle, and then the extract was centrifuged at high speed (14,000 rpm, 15 min). The pellet containing the membrane-derived protein fraction was solubilized using 1% DDM in HBS buffer for 1 h on ice, and the solution was ultracentrifuged at 30,000 rpm for 1 h. The membrane protein fraction was collected from the supernatant and subjected to the BCA protein assay.

Immunoprecipitation. Total membrane protein extracts were preabsorbed with anti-rabbit IgG-beads for 30 min. The precleared membrane protein extracts were then incubated with 2 to 5 μg of anti-$P2X_4$ or anti-$P2X_7$ antibody in HBS buffer containing 1% DDM for 2 h at 4°C. Anti-rabbit IgG beads were subsequently added to the samples, and the mixture was further incubated for 1 h at 4°C. The protein beads complexes were washed four times with HBS buffer containing 1% DDM, and proteins were eluted by boiling for 5 min in 40 μl of Laemmli buffer. Samples were analyzed by SDS-PAGE and were probed by Western blot using the corresponding primary antibody and Rabbit TrueBlot-HRP anti-rabbit IgG as secondary antibody. When the immunoprecipitation was performed using a monoclonal anti-HA antibody, protein G beads were used instead to isolate the complexes, and an HRP-anti-mouse secondary antibody was used for detection in Western blots.

Electrophysiological Recordings. Standard whole-cell recordings were performed at room temperature using an Axopatch 200A amplifier (Molecular Devices, Sunnyvale, CA). Patch pipettes (3–6 MΩ) were pulled from thick-walled borosilicate glass (GC150F-10; Harvard Apparatus, Inc., Holliston, MA). ATP-induced responses were measured at −30 mV, and different extracellular (EC) solutions

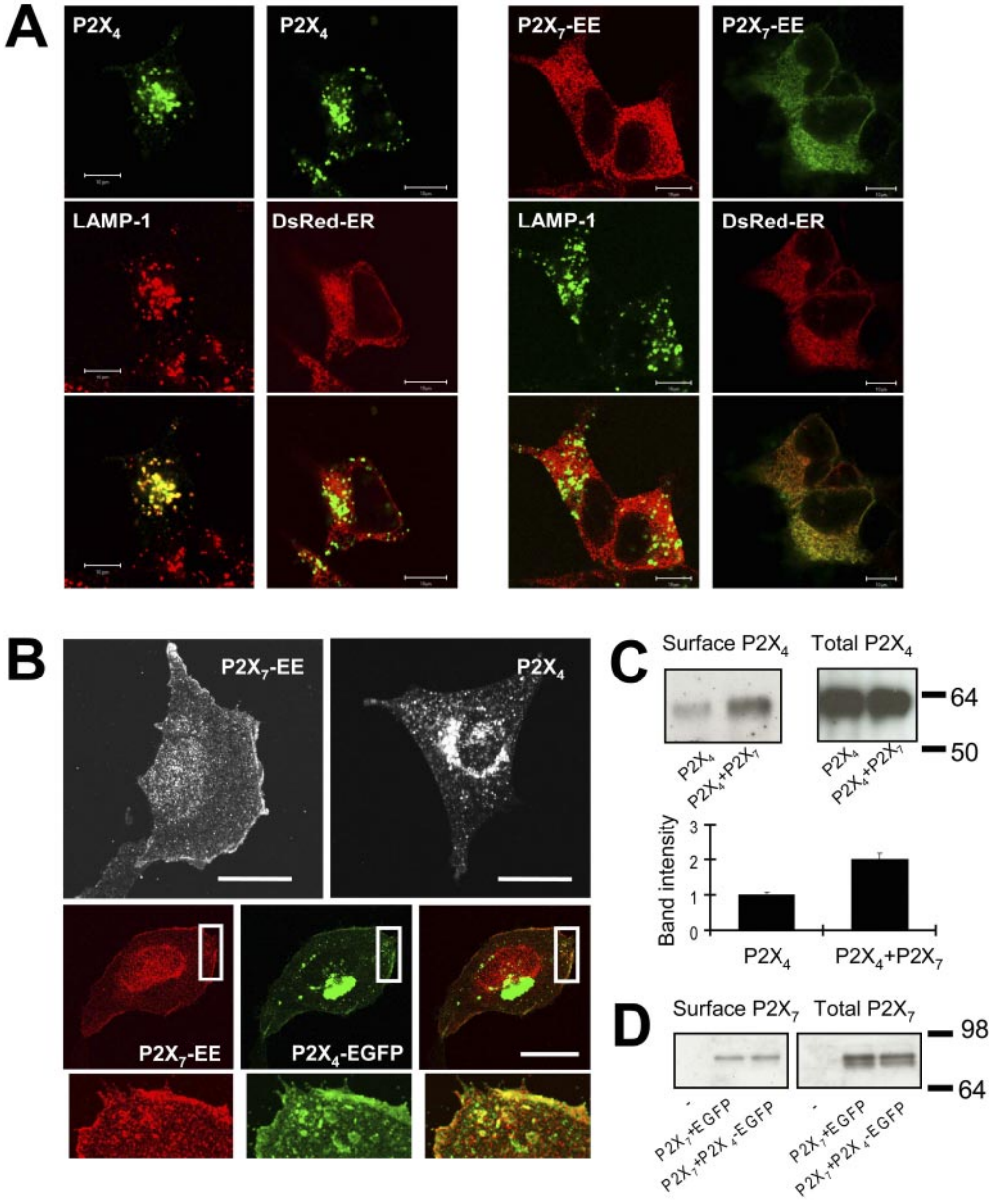

Fig. 1. Coexpression of $P2X_7$ and $P2X_4$ increased $P2X_4$ at the plasma membrane. A, confocal images of HEK293 cells transfected with either $P2X_4$ or $P2X_7$. $P2X_4$ receptors (green) were colocalized with LAMP-1 (red), and $P2X_7$ receptors (green) were colocalized with an ER marker, DsRed-ER. Cells were fixed with 3% PFA and permeabilized with 0.1% Triton X-100 in PBS for 10 min at 4°C. B, NRK cells transfected with either $P2X_7$ or $P2X_4$ alone (top) or cotransfected with $P2X_7$ and $P2X_4$-EGFP (bottom) were fixed with 100% methanol. Methanol fixation increased the detection of $P2X_7$ at the plasma membrane. In cotransfected cells, there was overlap between $P2X_4$ and $P2X_7$ at the plasma membrane. Scale bars, 10 μm. C, transfected NRK cells were incubated with biotin (1 mg/ml) for 20 min at 4°C to label surface proteins and were then solubilized, and surface proteins were precipitated with streptavidin beads. Surface expression of $P2X_4$ increased in the presence of $P2X_7$ (n = 4), although totals show equivalent $P2X_4$ expression. D, surface expression of $P2X_7$ was unchanged in the presence of $P2X_4$; in both cases, the proportion biotinylated was ~10% of the total $P2X_7$. The first lane shows no detectable expression of $P2X_7$ in untransfected cells.

were used. These included normal Na^+ EC solution (140 mM NaCl, 5 mM KCl, 2 mM $CaCl_2$, 1 mM $MgCl_2$, 10 mM D-glucose, and 10 mM HEPES, pH 7.3); Na^+ EC solution with low divalent (151 mM NaCl, 0.3 mM $CaCl_2$, 10 mM HEPES, and 10 mM glucose, pH 7.3); Cs^+ EC solution with low divalent (151 mM CsCl, 0.3 mM $CaCl_2$, 10 mM HEPES, and 10 mM glucose, pH 7.3); Cs^+ EC solution with 1.58 mM Ca^{2+} (151 mM CsCl, 1.58 mM $CaCl_2$, 10 mM HEPES, and 10 mM glucose, pH 7.3); Cs^+ plus Na^+ EC solution with low divalent (121 mM CsCl, 30 mM NaCl, 0.3 mM $CaCl_2$, 10 mM HEPES and 10 mM glucose, pH 7.3). When using Na^+ EC solution, the intracellular solution had the following composition (70 mM K_2SO_4, 10 mM KCl, 1 mM $MgCl_2$, 10 mM HEPES, and 75 mM sucrose, pH 7.3). When using a Cs^+ EC solution, the composition of the intracellular solution was as follows (151 mM CsCl, 10 mM HEPES, and 0.1 mM EGTA, pH 7.3).

Whole-cell currents were low pass-filtered at 2 kHz and digitized at 10 kHz. Agonists were applied locally using a Picospritzer II (Parker Hannifin, Mayfield Heights, OH). To ensure delivery of drug, 0.05% (w/v) fast green was used. (Local applications of 1% fast green induced no response.) To visualize cells expressing P2X receptors without an EGFP tag, cells were cotransfected with EGFP. Cells expressing EGFP or EGFP-tagged P2X subunits were observed under a microscope with an epifluorescence attachment (Nikon, Tokyo, Japan). Untransfected cells and cells expressing EGFP alone were found to have no inward current in response to application of agonists. Acquisition was performed using HEKA Pulse Version 8.30, and data were subsequently analyzed using IgorPRO Version 3.16. Statistical analyses were performed with Student's unpaired *t* test.

Results

Coexpression of $P2X_4$ and $P2X_7$ Increased the Surface Expression of $P2X_4$. We examined the distribution of $P2X_4$ and $P2X_7$ when expressed either individually or together in HEK293 and NRK cells using immunocytochemical labeling. We showed previously that $P2X_4$ receptors undergo rapid and constitutive endocytosis and reside predominantly within intracellular compartments (Bobanovic et al., 2002; Royle et al., 2002). Figure 1 shows $P2X_4$ colocalized with the lysosomal marker, Lamp-1, whereas $P2X_7$ receptors containing a Glu-Glu tag at the C terminus ($P2X_7$-EE) were predominantly colocalized with the ER marker, DsRed-ER (Fig. 1A). Using methanol rather than PFA to fix the cells, enhanced antibody labeling of $P2X_7$ was performed at the plasma membrane (Fig. 1B). When $P2X_4$ and $P2X_7$ were coexpressed in NRK cells, $P2X_4$ was still predominantly within endolysosomes, and there was very little labeling of $P2X_7$-EE in these compartments, suggesting that these receptors are $P2X_4$ homomers. At the plasma membrane, however, there was overlap in the distribution of the two receptors. To look at any change in the surface expression of $P2X_4$ and $P2X_7$, surface proteins were biotinylated and analyzed by Western blot (Fig. 1, C and D). The biotinylated fraction of $P2X_4$ increased ~2-fold in the presence of $P2X_7$, although total $P2X_4$ levels did not change, suggesting that association with $P2X_7$ stabilizes $P2X_4$ at the plasma membrane. In contrast, there was no change in the surface expression of $P2X_7$ with and without $P2X_4$.

Association of $P2X_4$ and $P2X_7$ Receptor Subunits. To test whether $P2X_7$ receptor subunits can associate with $P2X_4$ receptor subunits, we performed immunoprecipitation experiments using HEK293 cells cotransfected with $P2X_7$ and $P2X_4$. Membrane proteins were solubilized using 1% DDM because this was more effective at solubilizing $P2X_7$ than 1% Triton X-100, NP-40, or CHAPS (data not shown). After immunoprecipitation of the receptor complex using anti-$P2X_4$ antibody, $P2X_7$ was detected by immunoblotting with anti-$P2X_7$ antibody (Fig. 2A) but only when $P2X_4$ was also present. We also coexpressed $P2X_4$-HA with $P2X_7$ and were able to coimmunoprecipitate $P2X_7$ with anti-HA antibody (Fig. 2B). This gel shows that although two bands were detected for $P2X_7$ in the membrane fraction, which presumably represent fully and partially glycosylated forms, only the higher band was detected after coimmunoprecipitation. This suggests that the complex formed by $P2X_4$ and $P2X_7$ is not a misaggregate that is retained in the ER but instead is trafficked along the secretory pathway to the

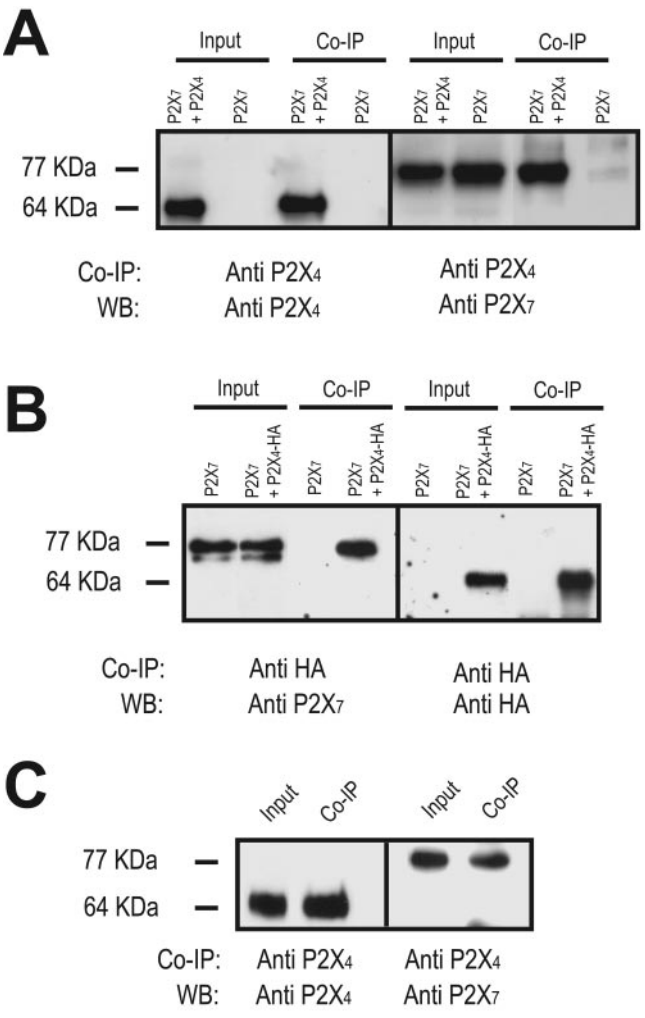

Fig. 2. $P2X_7$ and $P2X_4$ subunits physically associate both when overexpressed in HEK293 cells and in native tissue, as shown by coimmunoprecipitation. A, HEK293 cells were transfected with $P2X_4$ and $P2X_7$ or with $P2X_7$ alone, and membrane protein complexes were immunoprecipitated with the anti-$P2X_4$ antibody, separated by SDS-PAGE, and immunoblotted with anti-$P2X_4$ (left) and anti-$P2X_7$ (right) polyclonal antibodies. The total membrane protein fractions (input, 2.5 μg) were also blotted with the same antibodies for comparison. B, cells were cotransfected with $P2X_4$-HA and $P2X_7$ or with $P2X_7$ alone, and membrane proteins were immunoprecipitated with an anti-HA antibody, showing that the complex can be isolated via a non–P2X-specific antibody. Blots were performed with anti-$P2X_7$ (left) and anti-HA (right) antibodies. C, membrane protein fractions isolated from mice BMDMs were subjected to immunoprecipitation with the anti-$P2X_4$ antibody, and the isolated complex was resolved by SDS-PAGE and blotted with both anti-$P2X_4$ (left) and anti-$P2X_7$ (right) antibodies, demonstrating the physical association between $P2X_4$ and $P2X_7$ in native tissue.

trans-Golgi network and presumably from there to the plasma membrane.

Having shown that overexpressed $P2X_4$ and $P2X_7$ associate with one another, we next tested whether the endogenous receptors in bone marrow-derived macrophages could be coimmunoprecipitated. We performed the coimmunoprecipitation with anti-$P2X_4$ and the immunoblot with anti-$P2X_7$ and were able to detect a clear band running at the appropriate size for $P2X_7$ (Fig. 2C). Thus, native $P2X_4$ and $P2X_7$ receptors in mouse macrophages associate to form part of the same complex.

A Functional Interaction between $P2X_4$ and $P2X_7$ Receptors. To investigate the functional significance of the interaction between $P2X_4$ and $P2X_7$ subunits, we used two nonfunctional $P2X_4$ receptor mutants, C353W and S341W, which were characterized previously in *Xenopus laevis* oocytes (Silberberg et al., 2005). When expressed alone in oocytes, neither mutant produced a current in response up to 300 μM ATP, although their surface expression was equivalent to the wild-type (wt) $P2X_4$ receptor, indicating that the mutations interfered with channel functional and not maturation or trafficking. When coexpressed with wt $P2X_4$, the C353W mutant dramatically reduced the currents, whereas the S341W mutant had no inhibitory effect (Silberberg et al., 2005). We obtained very similar results using the EGFP-tagged mutants, expressed alone or with wt $P2X_4$ in HEK293 cells (Fig. 3A). Both mutants expressed individually were nonfunctional in response to 30 to 100 μM ATP, and when coexpressed with wt $P2X_4$, the C353W mutant reduced the peak current amplitude by ~75%, whereas the S341W mutant produced a small but not significant potentiation. We next compared the effect of these mutants on the current carried by the wt $P2X_7$ receptor (Fig. 3B). The $P2X_4$C353W mutant inhibited the $P2X_7$ receptor currents evoked by 1 mM

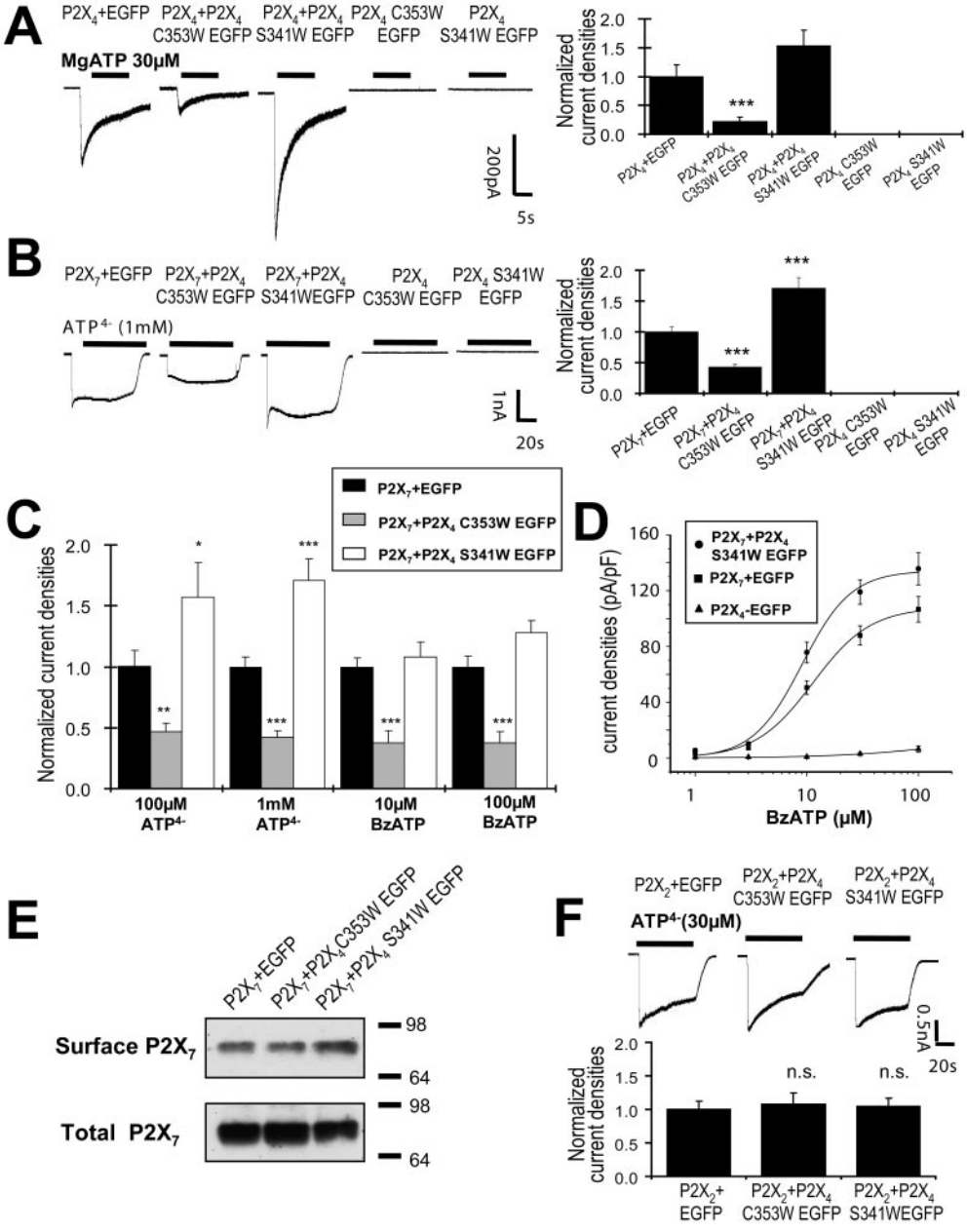

Fig. 3. Inhibition of $P2X_7$ receptor function by coexpression with a dominant-negative $P2X_4$ mutant. A, whole-cell patch-clamp recordings were carried out on HEK293 cells expressing $P2X_4$ alone or together with either the $P2X_4$C353W or $P2X_4$S341W mutants. The mutants were also expressed alone. Mutants were tagged with EGFP to enable the transfected cells to be detected. Inward currents, evoked by 30 μM MgATP at a holding potential of -30 mV, were measured in normal Na^+ EC solution. The histogram shows the normalized, mean peak current densities (mean $\pm$ S.E.M., $n > 8$). B, similar experiments were carried out, coexpressing $P2X_7$ and the $P2X_4$C353W and S341W mutants. Currents were evoked by applying 1 mM ATP^{4-} in Na^+ EC solution with a low divalent cation concentration at a holding potential of -30 mV. Histogram on the right shows a comparison of the normalized peak current densities (mean $\pm$ S.E.M., $n > 10$). C, similar results were obtained using either ATP^{4-} (100–1000 μM) or BzATP (10–100 μM). D, concentration-response curves for BzATP in HEK293 cells expressing $P2X_7$, $P2X_7$ and $P2X_4$ S341W, or $P2X_4$ alone. The data were fit with a Hill equation, and the EC_{50} values obtained were 11 $\pm$ 1 μM BzATP for $P2X_7$ and 9.1 $\pm$ 0.8 μM BzATP for $P2X_7$ with $P2X_4$ S341W ($n = 4$–7), and the corresponding Hill slopes were 1.7 $\pm$ 0.2 and 2.0 $\pm$ 0.3, respectively. E, the surface expression of $P2X_7$, as measured by biotinylation of surface proteins at 4°C, was unchanged in the presence of the two $P2X_4$ mutants. F, coexpression of the $P2X_4$ mutants with $P2X_2$ did not inhibit $P2X_2$-receptor mediated currents evoked by 30 μM ATP (mean $\pm$ S.E.M., $n > 10$). *, $p < 0.05$; **, $p < 0.01$; and ***, $p < 0.001$.

ATP^{4-} by greater than 50%, but the currents recorded from cells coexpressing the S341W mutant with $P2X_7$ were slightly increased compared with $P2X_7$ alone. Similar results were obtained with 100 μM ATP^{4-} and with the $P2X_7$ receptor preferred agonist, BzATP (Fig. 3C). We compared the BzATP dose-response relationship for $P2X_7$ alone and $P2X_7$ coexpressed with the S341W mutant, and the EC_{50} values were similar (11 $\pm$ 1 and 9.1 $\pm$ 0.8 μM, respectively) (Fig. 3D). In contrast, the wt $P2X_4$ receptor produced very little response to BzATP up to concentrations of 100 μM. Neither the S341W nor the C353W mutant altered the surface expression of $P2X_7$, as measured by biotinylating surface proteins (Fig. 3E), indicating that functional inhibition of $P2X_7$ by the C353W mutant was not caused by a reduction in the number of receptors reaching the plasma membrane. If we assume that association of the C353W mutant with $P2X_7$ abolishes receptor function, as suggested for receptors formed from wt $P2X_4$ and the C353W mutant, then we can estimate that there was a >2-fold reduction in the number of functional homomeric $P2X_7$ receptors at the plasma membrane in the presence of the C353W mutant. This suggests that more than half of the surface $P2X_7$ receptor subunits were associated with the $P2X_4$C353W mutant. In contrast to the inhibition of $P2X_7$ by $P2X_4$C353W, there was no change in $P2X_2$ receptor currents upon coexpression with either $P2X_4$C353W or S341W (Fig. 3F).

Having demonstrated an interaction between the $P2X_4$ mutants and wt $P2X_7$, we tested how coexpression of wt $P2X_4$ and $P2X_7$ affected the responses to BzATP and MgATP (Fig. 4, A and B). MgATP activated large currents in cells expressing $P2X_4$ alone, and BzATP activated large currents in cells expressing the $P2X_7$ receptor. In cells coexpressing these receptors, summation of the response produced by each receptor expressed individually would suggest two independent pools of homomeric receptors. The currents evoked by both agonists, however, were significantly reduced compared with what one would predict for a simple summation, suggesting a functional interaction between the two receptors. This was not the case for $P2X_2$ and $P2X_7$ (Fig. 4C), and the apparent lack of a functional interaction between these two subtypes was consistent with their inability to coimmunoprecipitate (Supplementary Fig. S1).

Coexpression of $P2X_4$ with $P2X_7$ Confers Ivermectin Sensitivity to BzATP-Evoked Currents. To further test whether or not an interaction between $P2X_4$ and $P2X_7$ alters the functional properties of the receptors, we compared some of their pharmacological properties when expressed individually and together. $P2X_7$ receptors have been shown to be sensitive to EC Na^+ (Ma et al., 2006). Substituting Cs^+ for Na^+ in the EC solution slowed the activation and deactivation kinetics of $P2X_7$ receptor currents and enhanced the difference in its time course compared with $P2X_4$ receptor currents (Fig. 5). It also potentiated the amplitude of both BzATP-evoked $P2X_7$ receptor currents and currents recorded

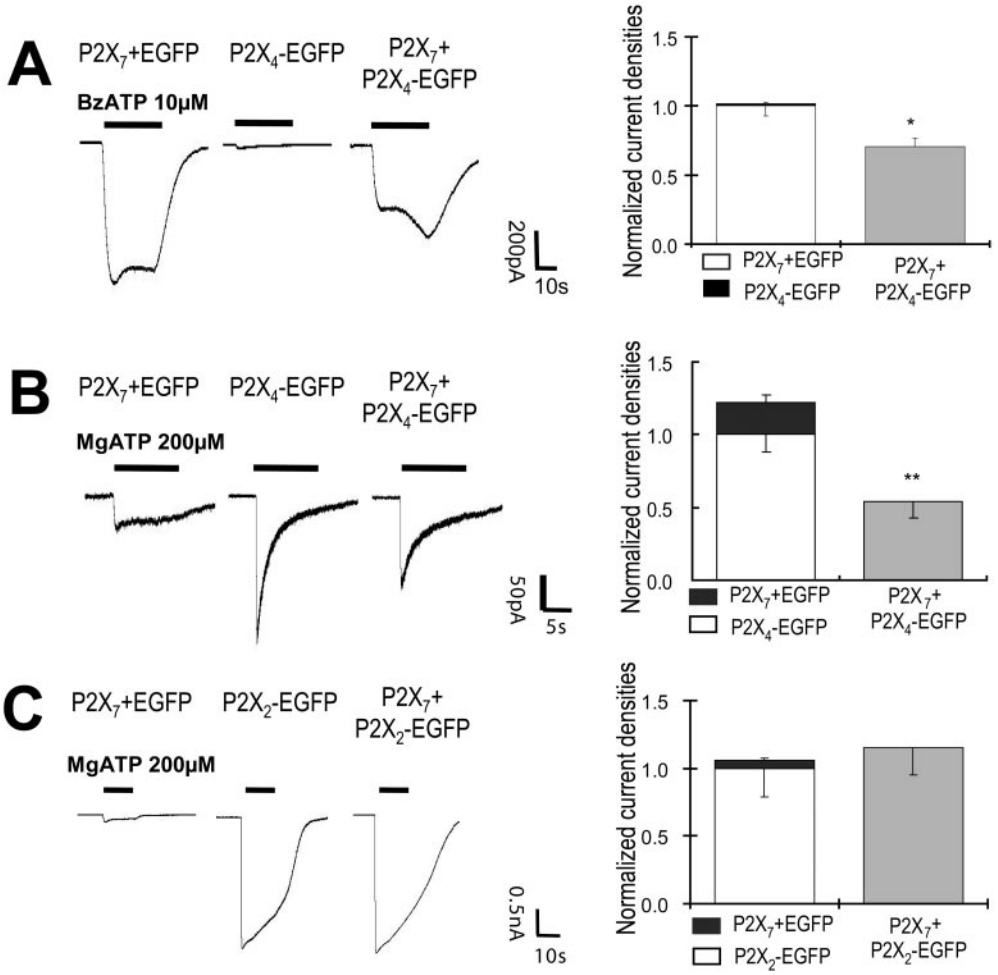

Fig. 4. $P2X_4$ but not $P2X_2$ functionally interacts with $P2X_7$. Whole-cell currents were recorded from HEK293 cells expressing the constructs shown. Normalized mean current densities are for $n > 8$ for each condition and $V_h = -30$ mV. A, inward currents were evoked by 10 μM BzATP in Na^+ EC solution with low divalent. B and C, inward currents were evoked by 200 μM MgATP in Na^+ EC solution with 1.58 mM Ca^{2+}.

from cells coexpressing $P2X_4$ and $P2X_7$ (Supplementary Fig. S2), whereas there was minimal activation of $P2X_4$ receptors using 3 μM BzATP (Fig. 5A). Ivermectin (IVM) is an allosteric modulator of $P2X_4$ receptors that augments currents by stabilizing the agonist-induced open state (Priel and Silberberg, 2004). We tested its effects on BzATP-evoked currents, and whereas there was no effect on currents from cells transfected with $P2X_7$ alone, in cells coexpressing $P2X_4$ and $P2X_7$, the currents were potentiated >2-fold after prior incubation with IVM. This suggests that association of $P2X_4$ with $P2X_7$ confers IVM sensitivity to the receptor, although this interpretation is confounded by the finding that BzATP is a much more effective agonist at homomeric $P2X_4$ receptors after IVM treatment. The time course of the $P2X_4$ receptor currents, however, differed from those recorded from cells coexpressing the two receptors. To remove any component of the whole-cell current that was mediated by $P2X_4$ homomeric receptors, a similar experiment was performed but using the $P2X_4$S341W mutant coexpressed with $P2X_7$. This mutant expressed alone was nonfunctional with and without IVM pretreatment but conferred IVM sensitivity to BzATP-evoked currents recorded from cells coexpressing this mutant with $P2X_7$ (Fig. 5B). Similar results were obtained with Na^+ EC solution (Fig. 5C) and using MgATP as the agonist, although the currents were much smaller (Fig. 5D).

TNP-ATP and Brilliant Blue G Inhibit $P2X_{4/7}$ Receptor Currents. We next tested the effects of the $P2X_4$ receptor antagonist, TNP-ATP, and the $P2X_7$ receptor antagonist Brilliant Blue G (BBG) (Virginio et al., 1998; Jiang et al., 2000; Tsuda et al., 2003). TNP-ATP (2 μM) inhibited MgATP-activated $P2X_4$ receptor currents by ~70% but had no significant effect on the amplitude of BzATP-evoked $P2X_7$ receptor currents. In contrast, it significantly inhibited BzATP-evoked currents from cells coexpressing $P2X_4$ and $P2X_7$ (Fig. 6A). At this concentration of BzATP, $P2X_4$ homomeric receptor currents are not expected to make a significant contribu-

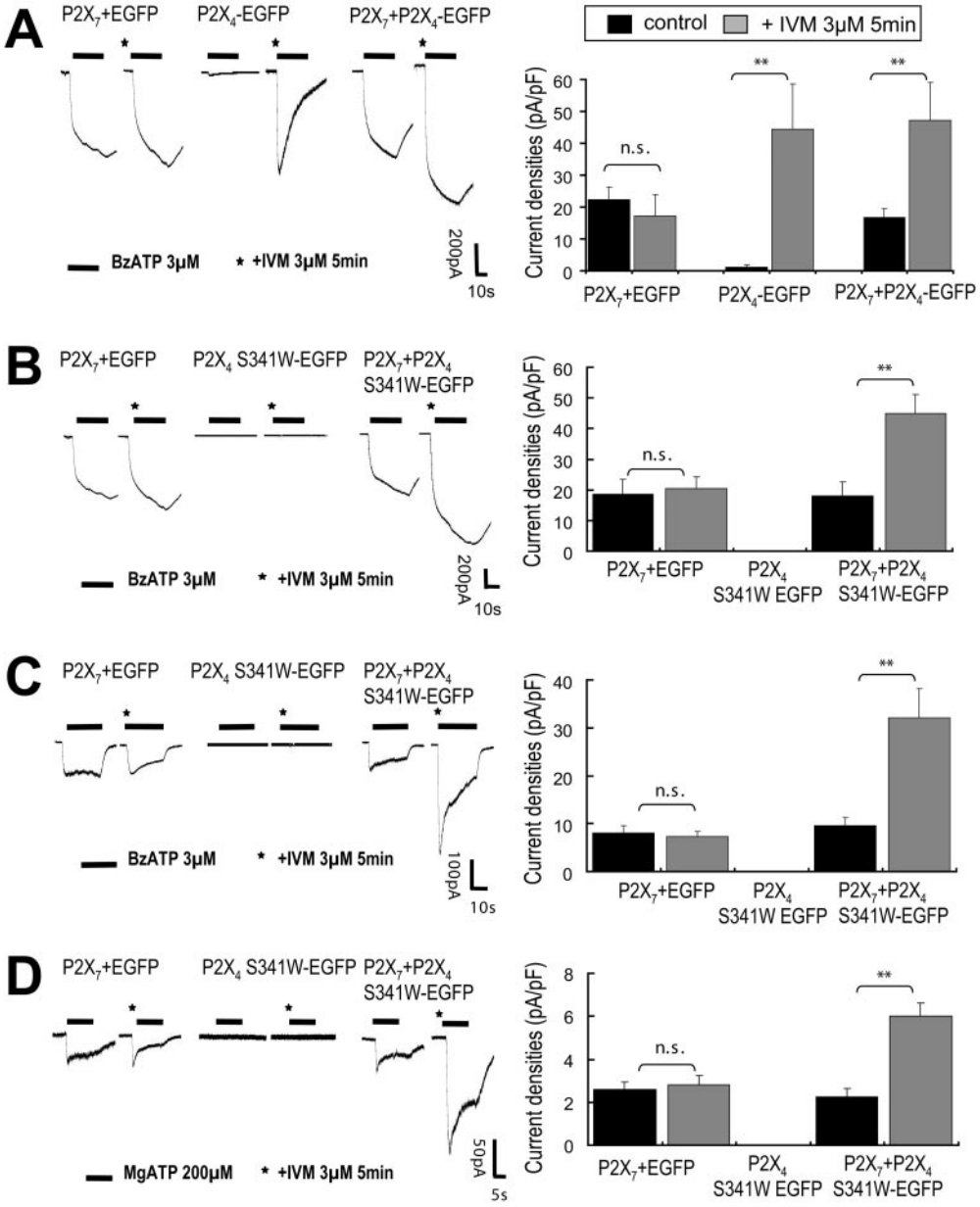

Fig. 5. $P2X_{4/7}$ receptor currents were potentiated by IVM. Whole-cell patch-clamp recordings from HEK293 cells expressing the constructs indicated with and without preincubation with 3 μM IVM for 5 min. $V_h = -30$ mV. All histograms represent peak current densities (mean ± S.E.M., $n > 10$). A and B, recordings were made in Cs^+ EC solution with low divalent cations in response to 3 μM BzATP. C, BzATP-activated currents were recorded in Na^+ EC solution with low divalent cations. D, currents were recorded in Na^+ EC solution containing 1.58 mM Ca^{2+} and in response to 200 μM MgATP.

tion to the whole-cell current amplitude; however, to rule out the possibility that there was a significant $P2X_4$ receptor-mediated component, the experiment was repeated using the S341W mutant. Currents recorded from cells coexpressing $P2X_4$ S341W and $P2X_7$ were reduced by ~70% after incubation with TNP-ATP.

Finally, we tested the effects of BBG, which almost completely abolished BzATP-activated $P2X_7$ receptor currents but had very little effect at $P2X_4$ receptors (Fig. 6B). It substantially reduced currents recorded from cells coexpressing $P2X_7$ and $P2X_4$ S341W, although these were significantly less sensitive as judged by the amplitude of the BzATP-evoked response after a 10-min incubation with 1 μM BBG.

Discussion

The $P2X_7$ receptor represents an important therapeutic target in a number of diseases such as stroke and arthritis pain. ATP-mediated responses in native tissues are frequently ascribed to $P2X_7$; however, they often display characteristics that are shared by other P2X receptors (North, 2002; Inoue, 2006). A molecular basis for these responses has not been established because the $P2X_7$ receptor is not believed to associate with any other P2X subunits. Our results provide evidence that the $P2X_7$ receptor can associate with another P2X subunit, which has an emerging role in pain and inflammation, namely $P2X_4$ (Tsuda et al., 2003; Inoue et al., 2004; Guo and Schluesener, 2005). This interaction was demonstrated not only in HEK293 cells overexpressing both receptors but also endogenously for native receptors present in primary cultures of BMDMs. Our results differ from those of an earlier study, which failed to coimmunoprecipitate $P2X_4$ and $P2X_7$ from HEK293 cells (Torres et al., 1999). A possible explanation is the use of different detergents; we used DDM, which often preserves protein activity better than other detergents, including NP-40. The association with $P2X_7$ affected the trafficking properties of $P2X_4$, increasing its stability at the plasma membrane, although it was still predominantly located within intracellular compartments. Coexpression with a dominant-negative mutant of $P2X_4$ (C353W) knocked down $P2X_7$ receptor currents by >50% without reducing its surface expression, suggesting that more than half of the surface $P2X_7$ subunits were in complexes associated with the C353W mutant. By using a nonfunctional but non–dominant-negative $P2X_4$ mutant,

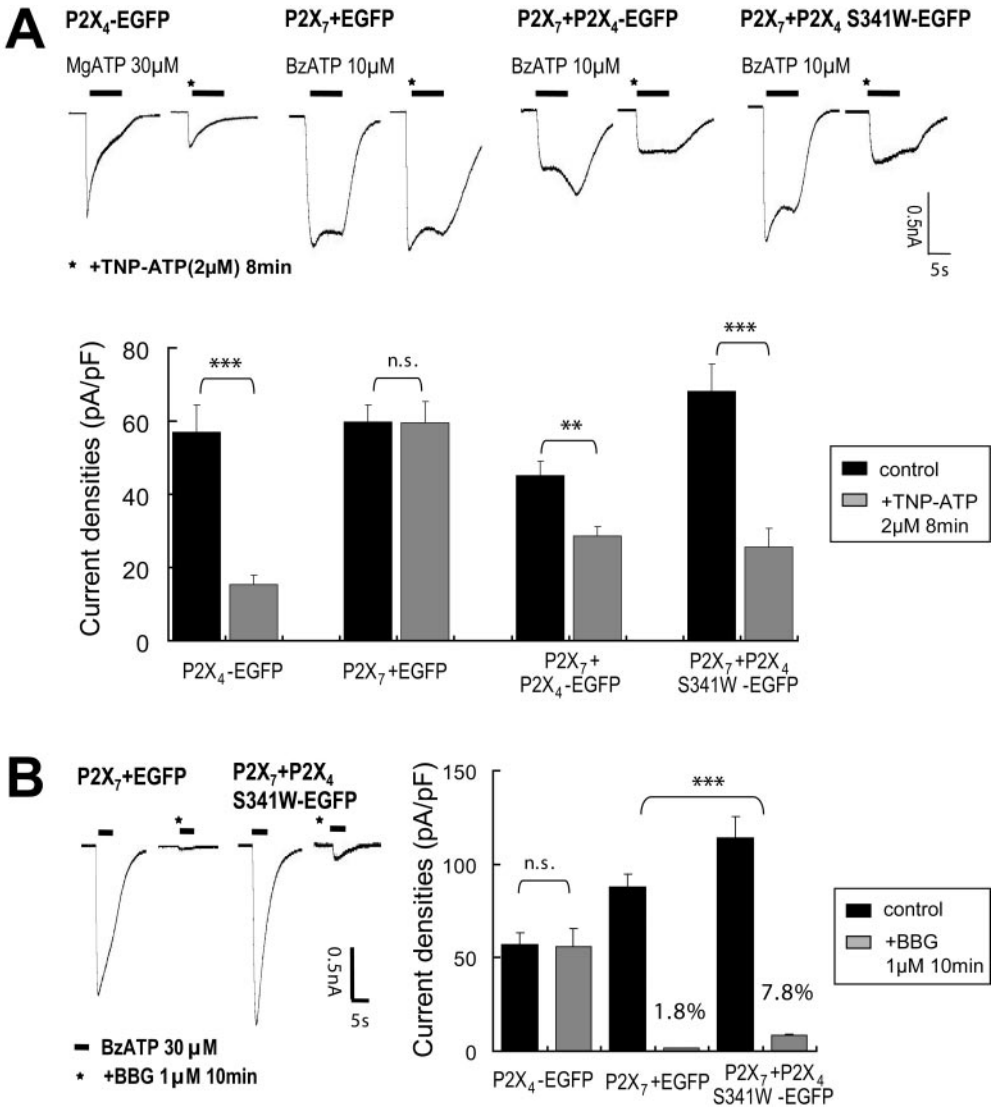

Fig. 6. Inhibition of $P2X_{4/7}$ receptor currents by TNP-ATP and BBG. A, whole-cell currents recorded in Na^+ EC solution, with and without preincubation with 2 μM TNP-ATP for 8 min. V_h = −30 mM. Histogram shows the peak current amplitudes (mean ± S.E.M., n >10). B, representative currents recorded from HEK293 cells expressing either $P2X_7$ or with $P2X_4$ S341W EGFP in response to 30 μM BzATP in Na^+ ES solution with low divalent. BBG (1 μM) was applied for 10 min. V_h = −30 mM. Histogram shows mean current densities ± S.E.M. The data for $P2X_4$ was obtained using 30 μM MgATP (n > 4) instead of BzATP.

we provide evidence that a heteromer formed from $P2X_4$ and $P2X_7$ has properties in common with both of the parent homomeric receptors. A question that remains to be answered is whether or not $P2X_4$ and $P2X_7$ subunits coassemble to form heterotrimeric structures with a common central conduction pore. In light of our findings, however, the prevailing hypothesis of $P2X_7$ receptors as unique members within the P2X family forming exclusively stable homotrimers seems unlikely to be correct.

The identification of novel functional properties that cannot be attributed to the parent homomeric receptors is a well-established approach for demonstrating heteromerization between different members of the same family of receptor. In this study, to distinguish between homomeric and heteromeric receptor currents, we took advantage of a $P2X_4$ receptor mutant (S341W), which, although nonfunctional when expressed alone, had been shown previously to traffic to the surface in the normal way and to produce no inhibition of wt $P2X_4$ receptor currents (Silberberg et al., 2005). When coexpressed with wt $P2X_7$, this mutant produced a small potentiation of BzATP- and ATP^{4-}-evoked currents, and we have made the assumption that currents with $P2X_4$-like pharmacological properties were mediated by a heteromer composed of $P2X_4$S341W and $P2X_7$. Our conclusions are that the heteromeric receptors are preferentially activated by BzATP compared with MgATP, they are allosterically modulated by IVM, and they are inhibited by both TNP-ATP and BBG. In Cs^+ EC solution, the IVM-sensitive component of the whole-cell current was larger in amplitude and with slower activation and deactivation kinetics than in Na^+ EC solution, suggesting that the $P2X_{4/7}$ complex is inhibited by EC Na^+ similar to $P2X_7$ homomeric receptors. The increase in receptor diversity as a result of functional heteromeric and homomeric P2X receptors being expressed in cells such as macrophages and microglia, which predominantly express $P2X_4$ and $P2X_7$, clearly has implications for the development of new therapies that target purinergic receptors for the treatment of neuropathic pain.

$P2X_4$ and $P2X_7$ are coexpressed in epithelial and endothelial cells and in immune cells (Bowler et al., 2003; Xiang and Burnstock, 2005; Ma et al., 2006). In airway epithelia, P2X receptor agonists stimulate Cl^- transport across nasal mucosa and are involved in the regulation of ciliary beat (Zsembery et al., 2004; Hayashi et al., 2005). Manipulation of both of these processes may be of therapeutic benefit for patients with cystic fibrosis, and defining the subunit identity and functional properties of the native receptors is important if these receptors are to be targeted for cystic fibrosis therapy. Ma et al. (2006) described the pharmacological features of the P2X receptor in airway ciliated cells, and several properties are similar to what we report here for the heterologously coexpressed receptors. The native receptor currents were inhibited by BBG and EC Na^+ and augmented by IVM. Based on this pharmacological profile, they hypothesized that the P2X receptor in ciliated cells is an assembly of $P2X_4$ and $P2X_7$ subunits, which is supported by our results.

The association between $P2X_4$ and $P2X_7$ may alter downstream signaling pathways, for example activation of the mitogen-activated protein kinase cascade (Donnelly-Roberts et al., 2004), phosphatidylserine translocation (Dutot et al., 2006), and coupling to ABC transporters (Marty et al., 2005). The hemichannel pannexin-1 was shown recently to form a complex with $P2X_7$ and to play an important role in coupling activation of the receptor to increased membrane permeability to large molecules such as ethidium and to IL-1β synthesis and release (Pelegrin and Surprenant, 2006). Whether pannexin-1 can functionally couple with $P2X_{4/7}$ receptors remains to be established. Our results provide a molecular basis for the existence of $P2X_{4/7}$ receptors, and further studies are required to elucidate the precise nature of the interaction between the constitutive subunits. These data also present functional significance for the heteromeric assembly between $P2X_4$ and $P2X_7$, and we foresee the importance of this interaction in purinergic receptor-mediated signaling of pain in health and disease.

Acknowledgments

We gratefully acknowledge the assistance of A. Paramasivam in the preparation of BMDMs cells.

References

Barrera NP, Ormond SJ, Henderson RM, Murrell-Lagnado RD, and Edwardson JM (2005) Atomic force microscopy imaging demonstrates that P2X2 receptors are trimers but that P2X6 receptor subunits do not oligomerize. *J Biol Chem* **280:** 10759–10765.

Bobanovic LK, Royle SJ, and Murrell-Lagnado RD (2002) P2X receptor trafficking in neurons is subunit specific. *J Neurosci* **22:**4814–4824.

Bowler JW, Bailey RJ, North RA, and Surprenant A (2003) P2X4, P2Y1 and P2Y2 receptors on rat alveolar macrophages. *Br J Pharmacol* **140:**567–575.

Chessell IP, Hatcher JP, Bountra C, Michel AD, Hughes JP, Green P, Egerton J, Murfin M, Richardson J, Peck WL, et al. (2005) Disruption of the P2X7 purinoceptor gene abolishes chronic inflammatory and neuropathic pain. *Pain* **114:**386–396.

Dell'Antonio G, Quattrini A, Dal Cin E, Fulgenzi A, and Ferrero ME (2002) Antinociceptive effect of a new P(2Z)/P2X7 antagonist, oxidized ATP, in arthritic rats. *Neurosci Lett* **327:**87–90.

Donnelly-Roberts DL, Namovic MT, Faltynek CR, and Jarvis MF (2004) Mitogen-activated protein kinase and caspase signaling pathways are required for P2X7 receptor (P2X7R)-induced pore formation in human THP-1 cells. *J Pharmacol Exp Ther* **308:**1053–1061.

Dutot M, Pouzaud F, Larosche I, Brignole-Baudouin F, Warnet JM, and Rat P (2006) Fluoroquinolone eye drop-induced cytotoxicity: role of preservative in P2X7 cell death receptor activation and apoptosis. *Invest Ophthalmol Vis Sci* **47:**2812–2819.

Gu BJ and Wiley JS (2006) Rapid ATP-induced release of matrix metalloproteinase 9 is mediated by the P2X7 receptor. *Blood* **107:**4946–4953.

Guo LH and Schluesener HJ (2005) Lesional accumulation of P2X(4) receptor(+) macrophages in rat CNS during experimental autoimmune encephalomyelitis. *Neuroscience* **134:**199–205.

Hayashi T, Kawakami M, Sasaki S, Katsumata T, Mori H, Yoshida H, and Nakahari T (2005) ATP regulation of ciliary beat frequency in rat tracheal and distal airway epithelium. *Exp Physiol* **90:**535–544.

Humphreys BD, Rice J, Kertesy SB, and Dubyak GR (2000) Stress-activated protein kinase/JNK activation and apoptotic induction by the macrophage P2X7 nucleotide receptor. *J Biol Chem* **275:**26792–26798.

Inoue K (2006) The function of microglia through purinergic receptors: neuropathic pain and cytokine release. *Pharmacol Ther* **109:**210–226.

Inoue K, Tsuda M, and Koizumi S (2004) ATP- and adenosine-mediated signaling in the central nervous system: chronic pain and microglia: involvement of the ATP receptor P2X4. *J Pharmacol Sci* **94:**112–114.

Jiang LH, Mackenzie AB, North RA, and Surprenant A (2000) Brilliant blue G selectively blocks ATP-gated rat $P2X_7$ receptors. *Mol Pharmacol* **58:**82–88.

Khakh BS and North RA (2006) P2X receptors as cell-surface ATP sensors in health and disease. *Nature* **442:**527–532.

King BF, Townsend-Nicholson A, Wildman SS, Thomas T, Spyer KM, and Burnstock G (2000) Coexpression of rat P2X2 and P2X6 subunits in *Xenopus* oocytes. *J Neurosci* **20:**4871–4877.

Kozak M (1987) At least six nucleotides preceding the AUG initiator codon enhance translation in mammalian cells. *J Mol Biol* **196:**947–950.

Labasi JM, Petrushova N, Donovan C, McCurdy S, Lira P, Payette MM, Brissette W, Wicks JR, Audoly L, and Gabel CA (2002) Absence of the P2X7 receptor alters leukocyte function and attenuates an inflammatory response. *J Immunol* **168:** 6436–6445.

Lewis C, Neidhart S, Holy C, North RA, Buell G, and Surprenant A (1995) Coexpression of P2X2 and P2X3 receptor subunits can account for ATP-gated currents in sensory neurons. *Nature* **377:**432–435.

Ma W, Korngreen A, Weil S, Cohen EB, Priel A, Kuzin L, and Silberberg SD (2006) Pore properties and pharmacological features of the P2X receptor channel in airway ciliated cells. *J Physiol* **571:**503–517.

Marty V, Medina C, Combe C, Parnet P, and Amedee T (2005) ATP binding cassette transporter ABC1 is required for the release of interleukin-1beta by P2X7-stimulated and lipopolysaccharide-primed mouse Schwann cells. *Glia* **49:**511–519.

Nicke A, Kerschensteiner D, and Soto F (2005) Biochemical and functional evidence for heteromeric assembly of P2X1 and P2X4 subunits. *J Neurochem* **92:**925–933.

North RA (2002) Molecular physiology of P2X receptors. *Physiol Rev* **82:**1013–1067.

Ormond SJ, Barrera NP, Qureshi OS, Henderson RM, Edwardson JM, and Murrell-Lagnado RD (2006) An uncharged region within the N terminus of the P2X6 receptor inhibits its assembly and exit from the endoplasmic reticulum. *Mol Pharmacol* **69:**1692–1700.

Pelegrin P and Surprenant A (2006) Pannexin-1 mediates large pore formation and interleukin-1beta release by the ATP-gated P2X7 receptor. *EMBO J* **25:**5071–5082.

Perregaux DG, McNiff P, Laliberte R, Conklyn M, and Gabel CA (2000) ATP acts as an agonist to promote stimulus-induced secretion of IL-1 beta and IL-18 in human blood. *J Immunol* **165:**4615–4623.

Priel A and Silbergberg SD (2004) Mechanism of ivermectin facilitation of human P2X4 receptor channels. *J Gen Physiol* **123:**281–293.

Royle SJ, Bobanovic LK, and Murrell-Lagnado RD (2002) Identification of a non-canonical tyrosine-based endocytic motif in an ionotropic receptor. *J Biol Chem* **277:**35378–35385.

Silberberg SD, Chang TH, and Swartz KJ (2005) Secondary structure and gating rearrangements of transmembrane segments in rat P2X4 receptor channels. *J Gen Physiol* **125:**347–359.

Torres GE, Egan TM, and Voigt MM (1999) Hetero-oligomeric assembly of P2X receptor subunits. Specificities exist with regard to possible partners. *J Biol Chem* **274:**6653–6659.

Tsuda M, Shigemoto-Mogami Y, Koizumi S, Mizokoshi A, Kohsaka S, Salter MW, and Inoue K (2003 P2X4 receptors induced in spinal microglia gate tactile allodynia after nerve injury. *Nature* **424:**778–783.

Virginio C, Robertson G, Surprenant A, and North RA (1998) Trinitrophenyl-substituted nucleotides are potent antagonists selective for P2X1, P2X3, and heteromeric P2X2/3 receptors. *Mol Pharmacol* **53:**969–973.

Wilson HL, Wilson SA, Surprenant A, and North RA (2002) Epithelial membrane proteins induce membrane blebbing and interact with the P2X7 receptor C terminus. *J Biol Chem* **277:**34017–34023.

Xiang Z and Burnstock G (2005) Expression of P2X receptors on rat microglial cells during early development. *Glia* **52:**119–126.

Zsembery A, Fortenberry JA, Liang L, Bebok Z, Tucker TA, Boyce AT, Braunstein GM, Welty E, Bell PD, Sorscher EJ, et al. (2004) Extracellular zinc and ATP restore chloride secretion across cystic fibrosis airway epithelia by triggering calcium entry. *J Biol Chem* **279:**10720–10729.

Address correspondence to: Dr. Ruth Murrell-Lagnado, Department of Pharmacology, University of Cambridge, Tennis Court Road, Cambridge CB2 1PD, United Kingdom. E-mail: rdm1003@cam.ac.uk